

See discussions, stats, and author profiles for this publication at: <https://www.researchgate.net/publication/6953010>

# Infrared Emission Spectra and Equilibrium Structures of Gaseous $\text{HgH}_2$ and $\text{HgD}_2$

ARTICLE in THE JOURNAL OF PHYSICAL CHEMISTRY A · DECEMBER 2005

Impact Factor: 2.69 · DOI: 10.1021/jp0540205 · Source: PubMed

CITATIONS

15

READS

32

3 AUTHORS, INCLUDING:



Alireza Shayesteh

University of Tehran

42 PUBLICATIONS 501 CITATIONS

SEE PROFILE



Shanshan Yu

NASA

126 PUBLICATIONS 1,003 CITATIONS

SEE PROFILE

Infrared Emission Spectra and Equilibrium Structures of Gaseous  $\text{HgH}_2$  and  $\text{HgD}_2$ 

Alireza Shayesteh, Shanshan Yu, and Peter F. Bernath\*

Department of Chemistry, University of Waterloo, Waterloo, ON, N2L 3G1, Canada

Received: July 20, 2005; In Final Form: September 15, 2005

A detailed analysis of the high-resolution infrared emission spectra of gaseous  $\text{HgH}_2$  and  $\text{HgD}_2$  in the 1200–2200  $\text{cm}^{-1}$  spectral range is presented. The  $\nu_3$  antisymmetric stretching fundamental bands of  $^{204}\text{HgH}_2$ ,  $^{202}\text{HgH}_2$ ,  $^{201}\text{HgH}_2$ ,  $^{200}\text{HgH}_2$ ,  $^{199}\text{HgH}_2$ ,  $^{198}\text{HgH}_2$ ,  $^{204}\text{HgD}_2$ ,  $^{202}\text{HgD}_2$ ,  $^{201}\text{HgD}_2$ ,  $^{200}\text{HgD}_2$ ,  $^{199}\text{HgD}_2$ , and  $^{198}\text{HgD}_2$ , as well as a few hot bands involving  $\nu_1$ ,  $\nu_2$ , and  $\nu_3$  were analyzed rotationally, and spectroscopic constants were obtained. Using the rotational constants of the 000, 100, 01<sup>1</sup>0, and 001 vibrational levels, we determined the equilibrium rotational constants ( $B_e$ ) of the most abundant isotopologues,  $^{202}\text{HgH}_2$  and  $^{202}\text{HgD}_2$ , to be 3.135325(24)  $\text{cm}^{-1}$  and 1.569037(16)  $\text{cm}^{-1}$ , respectively, and the associated equilibrium Hg–H and Hg–D internuclear distances ( $r_e$ ) are 1.63324(1) Å and 1.63315(1) Å, respectively. The  $r_e$  distances of  $^{202}\text{HgH}_2$  and  $^{202}\text{HgD}_2$  differ by about 0.005%, which can be attributed to the breakdown of the Born–Oppenheimer approximation.

## 1. Introduction

Mercury and its compounds have been studied extensively as toxic chemicals in the environment.<sup>1–5</sup> Two major anthropogenic sources of mercury in the environment are coal combustion and waste incineration.<sup>1</sup> Mercury in the atmosphere exists mainly as neutral Hg vapor, whereas mercuric salts and methyl–mercury compounds can be found in natural waters and sediments.<sup>4</sup> Anaerobic bacteria in natural waters can reduce Hg(II) to  $\text{Hg}^0$ , which is re-emitted to the atmosphere as vapor phase elemental mercury.<sup>5,6</sup> The reduction of Hg(II) to  $\text{Hg}^0$ , followed by the gas-phase detection of atomic mercury, is in fact a well-known method for detecting trace amounts of mercury in liquid and solid samples. The method is called “cold vapor generation”, which was developed in the late 1960s, and is based on the reduction of aqueous Hg(II) by  $\text{SnCl}_2$  or  $\text{NaBH}_4$  and detection of gas-phase  $\text{Hg}^0$  by atomic absorption spectroscopy.<sup>7,8</sup> A similar technique called “hydride generation” is based on the reduction of acidified solutions of group 13, 14, 15, and 16 elements by  $\text{NaBH}_4$  to form volatile hydrides, which can be detected in the gas phase after atomization.<sup>8</sup> The hydride generation technique was examined recently for mercury, and it was found that both atomic and molecular Hg species are formed in the reduction process.<sup>9</sup> Although this volatile mercury-containing molecule has not been identified, it might be  $\text{HgH}_2$ . In another experiment, methyl–mercury chloride ( $\text{CH}_3\text{HgCl}$ ) was reduced by  $\text{NaBH}_4$ , and the volatile  $\text{CH}_3\text{HgH}$  molecule was detected in the gas phase by FT-IR and mass spectrometry.<sup>10</sup> Considering the fact that anaerobic bacteria can reduce aqueous Hg(II) and aqueous ions of group 14, 15, and 16 elements to form volatile  $\text{Hg}^0$ ,  $\text{SnH}_4$ ,  $\text{PH}_3$ ,  $\text{AsH}_3$ , and  $\text{H}_2\text{S}$  in the environment,<sup>5,6,11,12</sup> a further reduction of  $\text{Hg}^0$  by these bacteria may result in formation of volatile  $\text{HgH}_2$ .

There have been several ab initio theoretical studies of the electronic structure and geometry of gaseous  $\text{HgH}_2$ , predicting a linear H–Hg–H structure and a closed-shell  $\tilde{X}^1\Sigma_g^+$  ground

electronic state.<sup>13–23</sup> The equilibrium Hg–H internuclear distances estimated by various theoretical models were in the range of 1.615–1.713 Å.<sup>13–22</sup> For a heavy atom like Hg, relativistic effects are significant and should be included in the calculations. Nonrelativistic calculations overestimate the Hg–H internuclear distance by more than 0.1 Å.<sup>13–18</sup> Harmonic vibrational frequencies of  $\text{HgH}_2$ ,  $\text{HgHD}$ , and  $\text{HgD}_2$  have been calculated at the DFT(B3LYP), MP2, and CCSD(T) levels of theory with relatively large basis sets.<sup>19–21</sup> Recently, Li et al.<sup>22</sup> performed a very high level ab initio calculation on this molecule and predicted the energies for many vibrational levels of  $\text{HgH}_2$ ,  $\text{HgHD}$ , and  $\text{HgD}_2$  for  $J = 0$  (no rotation) using a variational calculation. They also calculated that the gas-phase reaction:  $\text{Hg}(\text{g}) + \text{H}_2(\text{g}) \rightarrow \text{HgH}_2(\text{g})$  is endoergic by 20.8  $\text{kcal mol}^{-1}$  for ground-state ( $^1\text{S}$ ) mercury atoms.<sup>22</sup> The first excited state of Hg, the metastable  $^3\text{P}$  state, lies about 120  $\text{kcal mol}^{-1}$  above the ground state,<sup>24</sup> so the formation of gaseous  $\text{HgH}_2$  from the gas-phase reaction of  $\text{Hg}(^3\text{P})$  with  $\text{H}_2$  is highly exoergic.

The gas-phase reaction of excited mercury atoms  $\text{Hg}(^3\text{P})$  with molecular hydrogen has been studied by both theoretical calculations and laser pump–probe techniques.<sup>25–32</sup> The ground-state  $\text{Hg}(^1\text{S})$  does not react with  $\text{H}_2$  because of a high energy barrier, but excited mercury atoms in the  $^3\text{P}$  state can insert into the H–H bond and form the excited bent  $[\text{H}–\text{Hg}–\text{H}]^*$  complex.<sup>25–32</sup> This intermediate can dissociate into the  $\text{HgH}$  and H free radicals. The theoretical and experimental studies of this reaction were focused mainly on the production of  $\text{HgH}$  and H, and little attention was given to the formation of the ground-state linear H–Hg–H molecule in the gas phase.<sup>28</sup> The reactions of  $\text{H}_2$  with excited Mg, Zn, Cd, and Hg atoms have been reviewed by Breckenridge.<sup>32</sup>

Solid  $\text{HgH}_2$  was first synthesized in the 1950s, from the reaction of  $\text{HgI}_2$  with  $\text{LiAlH}_4$  in ether-THF-petroleum ether solution at  $-135^\circ\text{C}$ .<sup>33–35</sup> This solid was reported to be extremely unstable, decomposing at temperatures above  $-125^\circ\text{C}$ ,<sup>33–35</sup> and it is probably not possible to produce gaseous  $\text{HgH}_2$ .

\* Corresponding author. Department of Chemistry, University of Waterloo, 200 University Avenue West, Waterloo, ON, N2L 3G1, Canada. Tel: 519-888-4814. Fax: 519-746-0435. E-mail: bernath@uwaterloo.ca.

by heating the solid. Recently, Wang and Andrews<sup>21,36</sup> recorded the infrared spectra of solid  $\text{HgH}_2$ ,  $\text{HgHD}$ , and  $\text{HgD}_2$  and proposed that  $\text{HgH}_2$  forms a covalent molecular solid, unlike zinc and cadmium dihydrides.

Aldridge and Downs<sup>37</sup> have reviewed the chemical properties of group 12 and other main-group hydrides. Many transition-metal hydrides have been trapped in solid matrices at temperatures below 12 K and studied by infrared absorption spectroscopy.<sup>38</sup> Mercury dihydride has been formed in solid hydrogen, nitrogen, neon, and argon matrices from the reaction of excited mercury atoms with hydrogen.<sup>21,36,39,40</sup> The infrared absorption spectra of  $\text{HgH}_2$ ,  $\text{HgHD}$ , and  $\text{HgD}_2$  (trapped in solid matrices) were recorded, and vibrational frequencies of the infrared-active modes were obtained.<sup>21,36,39,40</sup>  $\text{HgH}_2$  has also appeared as a byproduct in the matrix isolation experiments designed to study the  $\text{HHgOH}$  and  $\text{Hg(OH)}_2$  molecules.<sup>41,42</sup>

We have reported the first observation of  $\text{HgH}_2$  and  $\text{HgD}_2$  molecules in the gas phase recently.<sup>43</sup> The molecules were generated by the reaction of mercury vapor with molecular hydrogen or deuterium in the presence of an electrical discharge and were identified unambiguously by their high-resolution infrared emission spectra. Rotational analysis of the antisymmetric stretching fundamental bands ( $\nu_3$ ) of  $\text{HgH}_2$  and  $\text{HgD}_2$  yielded the  $r_0$   $\text{Hg-H}$  and  $\text{Hg-D}$  internuclear distances.<sup>43</sup> Gaseous  $\text{ZnH}_2$ ,  $\text{ZnD}_2$ ,  $\text{CdH}_2$ , and  $\text{CdD}_2$  have also been studied in our laboratory, and detailed analyses of their high-resolution infrared emission spectra have been published.<sup>44–46</sup> A detailed analysis of all of the vibration–rotation bands observed in the infrared emission spectra of gaseous  $\text{HgH}_2$  and  $\text{HgD}_2$  is presented in this paper.

## 2. Experimental Section

The emission source used to generate gaseous  $\text{HgH}_2$  and  $\text{HgD}_2$  molecules has been described in our earlier paper.<sup>43</sup> A small zirconia boat containing about 100 g of mercury was placed inside the central part of an alumina tube. The tube contained stainless steel electrodes in both ends and was sealed with barium fluoride windows. Pure hydrogen or deuterium flowed slowly through the tube at room temperature, and the total pressure was held at 0.7 Torr using a rotary pump. A dc discharge (3 kV/333 mA) was created between the electrodes, and the resulting emission was focused onto the entrance aperture of a Bruker IFS 120 HR Fourier transform spectrometer using a barium fluoride lens. The infrared emission spectrum of  $\text{HgH}_2$  was recorded using a KBr beam splitter and an InSb detector cooled by liquid nitrogen. The spectral range was limited to 1750–2200  $\text{cm}^{-1}$  by the detector response and a 2200  $\text{cm}^{-1}$  long-wave pass filter. The instrumental resolution was set to 0.01  $\text{cm}^{-1}$  and, to improve the signal-to-noise ratio, 100 spectra were co-added during 90 min of recording. The spectrum of  $\text{HgD}_2$  was recorded using the same beam splitter and a liquid-nitrogen-cooled  $\text{HgCdTe}$  (MCT) detector. The spectral range for  $\text{HgD}_2$  was 1200–2200  $\text{cm}^{-1}$ , set by the transmission of the 2200  $\text{cm}^{-1}$  long-wave pass filter. The instrumental resolution was 0.01  $\text{cm}^{-1}$ , and 400 spectra were co-added during 6 h of recording. The signal-to-noise ratios for the strongest emission lines of  $\text{HgH}_2$  and  $\text{HgD}_2$  were about 100 and 40, respectively.

## 3. Results and Analysis

**3.1. Vibration–Rotation Bands.** The WSPECTRA program, written by M. Carleer (Université Libre de Bruxelles), was used to measure the line positions in  $\text{HgH}_2$  and  $\text{HgD}_2$  spectra. Emission lines of carbon monoxide (impurity) appeared in both

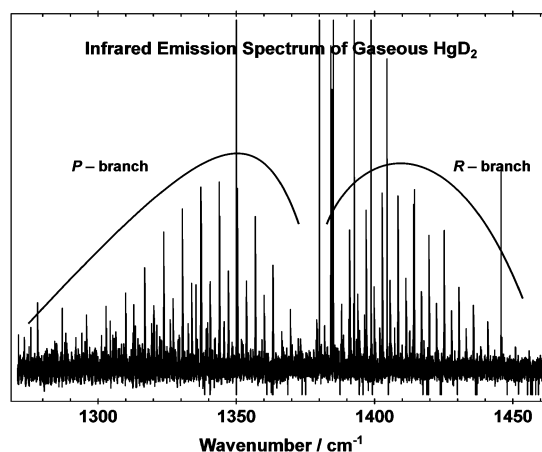


**Figure 1.** Overview of the infrared emission spectrum of gaseous  $\text{HgD}_2$  in the  $\nu_3$  region, recorded at a resolution of 0.01  $\text{cm}^{-1}$ .

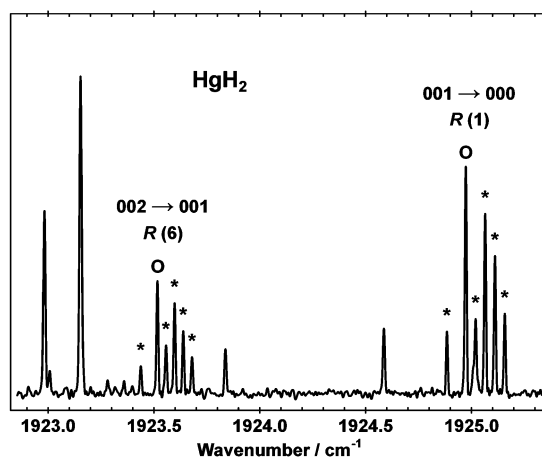


**Figure 2.** Very small portion of the  $\text{HgH}_2$  spectrum showing the isotope splitting in two  $R$ -branch lines of the  $001 \rightarrow 000$  and  $002 \rightarrow 001$  vibration–rotation bands. The lines marked with circles are from  $^{202}\text{HgH}_2$  and those marked with stars are from minor isotopes of mercury. The strong lines with no isotope splitting are from impurity CO.

spectra and were used for absolute wavenumber calibration.<sup>47</sup> The absolute accuracy of our calibrated line positions is better than 0.0005  $\text{cm}^{-1}$ . Rotational assignments of the vibration–rotation bands of  $\text{HgH}_2$  and  $\text{HgD}_2$  were facilitated using a color Loomis–Wood program.

An overview of the  $\text{HgD}_2$  spectrum is shown in Figure 1. Mercury has seven stable isotopes, and their terrestrial abundances are the following:  $^{204}\text{Hg}$  (6.9%),  $^{202}\text{Hg}$  (29.8%),  $^{201}\text{Hg}$  (13.2%),  $^{200}\text{Hg}$  (23.1%),  $^{199}\text{Hg}$  (16.9%),  $^{198}\text{Hg}$  (10.0%), and  $^{196}\text{Hg}$  (0.1%). Lines from six isotopes (all except  $^{196}\text{Hg}$ ) were observed in both spectra, and their intensity ratios match their natural abundances. Figure 2 is a very small portion of the  $\text{HgH}_2$  spectrum, showing the isotope splitting in two rotational lines. The adjacent rotational lines in  $\text{HgH}_2$  and  $\text{HgD}_2$  spectra had 3:1 and 1:2 intensity ratios, respectively, because of the ortho-para nuclear spin statistical weights associated with hydrogen ( $I = 1/2$ ) and deuterium ( $I = 1$ ) nuclei.<sup>48</sup> An expanded view of the  $\text{HgD}_2$  spectrum in Figure 3 shows the 1:2 intensity alternation. In addition to the  $\nu_3$  fundamental band, that is,  $001 (\Sigma_g^+) \rightarrow 000 (\Sigma_g^+)$ , the following hot bands were observed for  $^{202}\text{HgH}_2$ ,  $^{200}\text{HgH}_2$ ,  $^{202}\text{HgD}_2$ , and  $^{200}\text{HgD}_2$ :  $002 (\Sigma_g^+) \rightarrow 001 (\Sigma_u^+)$ ,  $003 (\Sigma_u^+) \rightarrow 002 (\Sigma_g^+)$ ,  $101 (\Sigma_u^+) \rightarrow 100 (\Sigma_g^+)$ , and  $01^1 1 (\Pi_g) \rightarrow 01^0 1 (\Pi_u)$ . Fewer hot bands were detectable for the other isotopes of mercury because of their lower abundances.

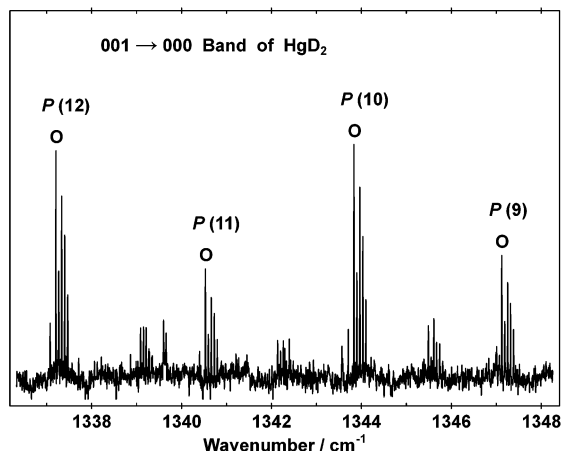


**Figure 3.** Expanded view of the  $\text{HgD}_2$  spectrum showing the 1:2 intensity alternation and the mercury isotope splitting in  $P$ -branch lines of the  $\nu_3$  fundamental band. The weaker lines are from the hot bands of  $\text{HgD}_2$ .

The vibrational energy of a linear triatomic molecule in the  $1\Sigma_g^+$  ground electronic state can be expressed by the following equation<sup>48</sup>

$$G(v_1, v_2, v_3) = \omega_1(v_1 + 1/2) + \omega_2(v_2 + 1) + \omega_3(v_3 + 1/2) + x_{11}(v_1 + 1/2)^2 + x_{22}(v_2 + 1)^2 + x_{33}(v_3 + 1/2)^2 + g_{22}l^2 + x_{12}(v_1 + 1/2)(v_2 + 1) + x_{13}(v_1 + 1/2)(v_3 + 1/2) + x_{23}(v_2 + 1)(v_3 + 1/2) \quad (1)$$

in which  $\omega_i$  values are the harmonic vibrational frequencies and  $x_{ij}$  values are second-order anharmonicity constants. The vibrational quantum numbers for the symmetric stretching ( $\sigma_g$ ), bending ( $\pi_u$ ), and antisymmetric stretching ( $\sigma_u$ ) modes are represented by  $v_1$ ,  $v_2$ , and  $v_3$ , respectively, and  $l$  is the vibrational angular momentum quantum number. The rotational energy for the  $\Sigma$  ( $l = 0$ ) and  $\Pi$  ( $l = 1$ ) states can be expressed by the following equation<sup>49</sup>

$$F_{[v]}(J) = B[J(J+1) - l^2] - D[J(J+1) - l^2]^2 \pm \frac{1}{2}[qJ(J+1) + q_D J^2(J+1)^2] \quad (2)$$

in which  $J$  is the total angular momentum quantum number (including rotation),  $B$  is the inertial rotational constant, and  $D$  is the centrifugal distortion constant. The rotational  $l$ -type doubling parameters,  $q$  and  $q_D$ , are nonzero only for the  $\Pi$  states, and the  $+$  ( $-$ ) sign refers to the  $e$  ( $f$ ) parity component.<sup>48</sup> An experimental uncertainty of  $0.0005 \text{ cm}^{-1}$  was used for the rotational lines of the  $001 \rightarrow 000$  fundamental band of  $\text{HgH}_2$  and  $\text{HgD}_2$ . Lines from the hot bands were less intense and were given an uncertainty of  $0.001 \text{ cm}^{-1}$ .

The absolute rotational assignments of the  $001 (\Sigma_u^+) \rightarrow 000 (\Sigma_g^+)$  fundamental bands of  $\text{HgH}_2$  and  $\text{HgD}_2$  were obtained easily because we observed all of the rotational lines near the band origins. The intensity ratios of adjacent rotational lines further confirmed our absolute  $J$  assignments. The rotational assignment of the  $002 (\Sigma_g^+) \rightarrow 001 (\Sigma_u^+)$  and  $003 (\Sigma_u^+) \rightarrow 002 (\Sigma_g^+)$  hot bands were obtained consecutively using lower state combination differences. All of the rotational lines of the  $001 (\Sigma_u^+) \rightarrow 000 (\Sigma_g^+)$ ,  $002 (\Sigma_g^+) \rightarrow 001 (\Sigma_u^+)$ , and  $003 (\Sigma_u^+) \rightarrow 002 (\Sigma_g^+)$  bands were fitted together using the energy expression in eq 2, and the spectroscopic constants were determined. A

complete list of the observed line positions for all isotopologues and the outputs of our least-squares fitting program have been placed in Tables 1S–12S, provided as Supporting Information. The spectroscopic constants for  $^{202}\text{HgH}_2$ ,  $^{200}\text{HgH}_2$ ,  $^{202}\text{HgD}_2$ , and  $^{200}\text{HgD}_2$  are presented in Tables 1 and 2, and those for the minor isotopes of mercury are in Tables 5S–12S. The ground-state vibrational energy ( $G_{000}$ ) was set to zero in the least-squares fitting, and the reported constants can reproduce the data within the experimental uncertainty ( $\sim 0.001 \text{ cm}^{-1}$ ).

One of the hot bands in both  $\text{HgH}_2$  and  $\text{HgD}_2$  spectra had large  $l$ -type doubling, and was assigned to the  $01^1 1 (\Pi_g) \rightarrow 01^1 0 (\Pi_u)$  transition. The absolute  $J$  assignment for this band was obtained based on the intensity alternation and the fact that  $e$  and  $f$  parity components of a  $\Pi$  state have the same vibrational band origins. Rotational lines of the  $01^1 1 (\Pi_g) \rightarrow 01^1 0 (\Pi_u)$  bands of  $\text{HgH}_2$  and  $\text{HgD}_2$  were fitted using the energy expression in eq 2 with  $l = 1$ . The vibrational energy of the  $01^1 0$  state was set to zero because we can only determine the difference between the  $01^1 1$  and  $01^1 0$  vibrational energies using our data. Rotational constants and the  $l$ -type doubling constants of the  $01^1 0$  and  $01^1 1$  states are reported in Tables 1 and 2 for  $^{202}\text{HgH}_2$ ,  $^{200}\text{HgH}_2$ ,  $^{202}\text{HgD}_2$ , and  $^{200}\text{HgD}_2$ .

The absolute  $J$  assignments of the  $101 (\Sigma_u^+) \rightarrow 100 (\Sigma_g^+)$  hot bands of  $\text{HgH}_2$  and  $\text{HgD}_2$  were difficult to obtain because a few rotational lines near the band origins were missing. Therefore, we had to estimate the rotational constants ( $B$ ) of the  $100 (\Sigma_g^+)$  states of  $\text{HgH}_2$  and  $\text{HgD}_2$  to obtain definite  $J$  assignments for these bands. Rotational constants ( $B$ ) of the  $000$ ,  $01^1 0$ , and  $001$  states were used to calculate the vibration–rotation interaction constants,  $\alpha_2$  and  $\alpha_3$ , for  $^{202}\text{HgH}_2$  and  $^{202}\text{HgD}_2$  using the following linear equation:<sup>48</sup>

$$B_{[v]} = B_e - \alpha_1(v_1 + 1/2) - \alpha_2(v_2 + 1) - \alpha_3(v_3 + 1/2) \quad (3)$$

Within the Born–Oppenheimer approximation, the ratio of the  $B_e$  values of  $^{202}\text{HgH}_2$  and  $^{202}\text{HgD}_2$  is simply given by

$$\frac{B_e(^{202}\text{HgH}_2)}{B_e(^{202}\text{HgD}_2)} = \frac{m_D}{m_H} \quad (4)$$

in which  $m_D$  and  $m_H$  are atomic masses of deuterium and hydrogen, respectively. In addition, a simple mass-scaling ratio exists for the  $\alpha_1$  constants of  $^{202}\text{HgH}_2$  and  $^{202}\text{HgD}_2$ :<sup>46,49</sup>

$$\frac{\alpha_1(^{202}\text{HgH}_2)}{\alpha_1(^{202}\text{HgD}_2)} = \left(\frac{m_D}{m_H}\right)^{3/2} \quad (5)$$

Using the  $B_{000}$ ,  $\alpha_2$ , and  $\alpha_3$  constants of both  $^{202}\text{HgH}_2$  and  $^{202}\text{HgD}_2$ , we were able to estimate  $\alpha_1$  and  $B_e$  for these isotopologues by taking advantage of their isotopic ratios, eqs 3–5. The absolute  $J$  assignments of the  $101 (\Sigma_u^+) \rightarrow 100 (\Sigma_g^+)$  hot bands of  $\text{HgH}_2$  and  $\text{HgD}_2$  were then obtained immediately because we had reasonable estimates for the  $\alpha_1$  constants. Rotational lines of the  $101 (\Sigma_u^+) \rightarrow 100 (\Sigma_g^+)$  hot bands were fitted using the energy expression in eq 2 with  $l = 0$ , and the unknown vibrational energy of the lower state ( $100, \Sigma_g^+$ ) was set to zero in the least-squares fitting (see Tables 1 and 2).

In our previous studies on  $\text{CdH}_2$  and  $\text{ZnH}_2$ , we observed local perturbations and Fermi resonance in some vibrational levels.<sup>45,46</sup> The  $001$  vibrational levels of  $\text{CdH}_2$  and  $\text{ZnH}_2$  were perturbed locally by the nearby  $030$  levels because  $\nu_3 \approx 3\nu_2$  for these molecules. Strong Fermi resonances were also observed between the  $002 (\Sigma_g^+)$  and  $200 (\Sigma_g^+)$  levels because  $\nu_3 \approx \nu_1$  for both



**TABLE 1: Spectroscopic Constants (in cm<sup>-1</sup>) of <sup>202</sup>HgH<sub>2</sub> and <sup>200</sup>HgH<sub>2</sub>**

molecule	state	$G_{[v]} - G_{000}$	$B$	$D/10^{-5}$	$q/10^{-2}$	$q_D/10^{-6}$
<sup>202</sup> HgH <sub>2</sub>	000 ( $\Sigma_g^+$ )	0.0	3.0848585(37) <sup>a</sup>	2.83129(76)		
	001 ( $\Sigma_u^+$ )	1912.81427(6)	3.0550309(34)	2.85675(63)		
	002 ( $\Sigma_g^+$ )	3795.38853(17)	3.0231248(40)	2.90922(94)		
	003 ( $\Sigma_u^+$ )	5637.39817(27)	2.9851048(58)	3.0813(19)		
	100 ( $\Sigma_g^+$ ) <sup>b</sup>	$\nu_1$	3.036964(32)	2.877(24)		
	101 ( $\Sigma_u^+$ )	1842.02415(30) + $\nu_1$	3.006489(32)	2.902(21)		
	01 <sup>1</sup> 0 ( $\Pi_u$ ) <sup>b</sup>	$\nu_2$	3.073253(13)	2.8634(53)	-4.3421(18)	1.56(8)
	01 <sup>1</sup> 1 ( $\Pi_g$ )	1896.67557(16) + $\nu_2$	3.043677(12)	2.8879(44)	-4.2410(17)	1.44(7)
<sup>200</sup> HgH <sub>2</sub>	000 ( $\Sigma_g^+$ )	0.0	3.0848578(39)	2.83101(92)		
	001 ( $\Sigma_u^+$ )	1912.90555(6)	3.0550265(36)	2.85688(78)		
	002 ( $\Sigma_g^+$ )	3795.56107(16)	3.0231103(41)	2.90782(98)		
	003 ( $\Sigma_u^+$ )	5637.62326(24)	2.9850824(55)	3.0864(19)		
	100 ( $\Sigma_g^+$ ) <sup>b</sup>	$\nu_1$	3.036962(67)	2.877(65)		
	101 ( $\Sigma_u^+$ )	1842.11402(53) + $\nu_1$	3.006467(68)	2.896(55)		
	01 <sup>1</sup> 0 ( $\Pi_u$ ) <sup>b</sup>	$\nu_2$	3.073263(18)	2.8634(88)	-4.3412(25)	1.46(14)
	01 <sup>1</sup> 1 ( $\Pi_g$ )	1896.76451(22) + $\nu_2$	3.043689(16)	2.8916(69)	-4.2402(23)	1.36(11)

<sup>a</sup> The numbers in parentheses are one standard deviation statistical uncertainties in the last quoted digits. <sup>b</sup> The wavenumbers of  $\nu_1$  and  $\nu_2$  could not be determined from our data. The best ab initio value (ref 22) for  $\nu_1$  is 1982 cm<sup>-1</sup>, and the neon matrix value (ref 21) for  $\nu_2$  is 782 cm<sup>-1</sup>.

**TABLE 2: Spectroscopic Constants (in cm<sup>-1</sup>) of <sup>202</sup>HgD<sub>2</sub> and <sup>200</sup>HgD<sub>2</sub>**

molecule	state	$G_{[v]} - G_{000}$	$B$	$D/10^{-5}$	$q/10^{-2}$
<sup>202</sup> HgD <sub>2</sub>	000 ( $\Sigma_g^+$ )	0.0	1.5511565(26) <sup>a</sup>	0.70542(24)	
	001 ( $\Sigma_u^+$ )	1375.78848(8)	1.5405124(26)	0.70959(25)	
	002 ( $\Sigma_g^+$ )	2736.90048(20)	1.5294338(30)	0.71714(36)	
	003 ( $\Sigma_u^+$ )	4080.50260(52)	1.5173166(77)	0.7377(21)	
	100 ( $\Sigma_g^+$ ) <sup>b</sup>	$\nu_1$	1.534289(21)	0.7105(51)	
	101 ( $\Sigma_u^+$ )	1340.11730(35) + $\nu_1$	1.523499(22)	0.7160(54)	
	01 <sup>1</sup> 0 ( $\Pi_u$ ) <sup>b</sup>	$\nu_2$	1.547031(10)	0.7126(20)	-1.52172(74)
	01 <sup>1</sup> 1 ( $\Pi_g$ )	1367.58606(21) + $\nu_2$	1.536456(10)	0.7188(23)	-1.49770(78)
<sup>200</sup> HgD <sub>2</sub>	000 ( $\Sigma_g^+$ )	0.0	1.5511599(31)	0.70558(31)	
	001 ( $\Sigma_u^+$ )	1375.91976(9)	1.5405104(31)	0.70937(31)	
	002 ( $\Sigma_g^+$ )	2737.15442(23)	1.5294221(36)	0.71603(45)	
	003 ( $\Sigma_u^+$ )	4080.85692(59)	1.5172882(90)	0.7297(24)	
	100 ( $\Sigma_g^+$ ) <sup>b</sup>	$\nu_1$	1.534306(21)	0.7108(44)	
	101 ( $\Sigma_u^+$ )	1340.24600(38) + $\nu_1$	1.523516(21)	0.7187(42)	
	01 <sup>1</sup> 0 ( $\Pi_u$ ) <sup>b</sup>	$\nu_2$	1.547042(13)	0.7130(28)	-1.52157(86)
	01 <sup>1</sup> 1 ( $\Pi_g$ )	1367.71516(25) + $\nu_2$	1.536455(14)	0.7167(34)	-1.49735(89)

<sup>a</sup> The numbers in parentheses are one standard deviation statistical uncertainties in the last quoted digits. <sup>b</sup> The wavenumbers of  $\nu_1$  and  $\nu_2$  could not be determined from our data. The best ab initio value (ref 22) for  $\nu_1$  is 1421 cm<sup>-1</sup>, and the neon matrix value (ref 21) for  $\nu_2$  is 562 cm<sup>-1</sup>.

CdH<sub>2</sub> and ZnH<sub>2</sub>.<sup>45,46</sup> In contrast, we did not observe similar perturbations in the vibration-rotation bands of HgH<sub>2</sub> and HgD<sub>2</sub>. Based on the harmonic vibrational frequencies predicted by Greene et al.,<sup>20</sup>  $\nu_1$  and  $3\nu_2$  are considerably larger than  $\nu_3$  for HgH<sub>2</sub> and HgD<sub>2</sub>, and the above perturbations are not expected.

**3.2. Determination of Internuclear Distances.** The  $B_{000}$  constants of <sup>202</sup>HgH<sub>2</sub>, <sup>200</sup>HgH<sub>2</sub>, <sup>202</sup>HgD<sub>2</sub>, and <sup>200</sup>HgD<sub>2</sub>, taken from Tables 1 and 2, were used to determine the  $r_0$  internuclear distances directly from the moment of inertia equation. The  $r_0$  values obtained for <sup>202</sup>HgH<sub>2</sub> and <sup>202</sup>HgD<sub>2</sub> are 1.646543(1) Å and 1.642535(2) Å, respectively. This discrepancy ( $\sim 0.004$  Å) is due to the fact that the 000 ground state of HgD<sub>2</sub> lies lower than that of HgH<sub>2</sub> on the potential energy surface. However, the  $r_0$  distances for different isotopes of mercury are equal within the statistical uncertainties.

By taking the differences between the ground-state rotational constant ( $B_{000}$ ) and the  $B_{[v]}$  values of the 100, 01<sup>1</sup>0, and 001

states, we determined the vibration-rotation interaction constants ( $\alpha_1$ ,  $\alpha_2$ , and  $\alpha_3$  in eq 3). The equilibrium rotational constants ( $B_e$ ) of <sup>202</sup>HgH<sub>2</sub>, <sup>200</sup>HgH<sub>2</sub>, <sup>202</sup>HgD<sub>2</sub>, and <sup>200</sup>HgD<sub>2</sub> were then calculated using their  $B_{000}$  values and the three  $\alpha$ 's. The equilibrium centrifugal distortion constant ( $D_e$ ) was calculated for these isotopologues using a linear equation analogous to eq 3 for the  $D_{[v]}$  values. Table 3 has a list of molecular constants determined for <sup>202</sup>HgH<sub>2</sub>, <sup>200</sup>HgH<sub>2</sub>, <sup>202</sup>HgD<sub>2</sub>, and <sup>200</sup>HgD<sub>2</sub> in this study. Using the  $B_e$  values of 3.135325(24) cm<sup>-1</sup> and 1.569037(16) cm<sup>-1</sup> for <sup>202</sup>HgH<sub>2</sub> and <sup>202</sup>HgD<sub>2</sub>, respectively, we determined the equilibrium internuclear distances ( $r_e$ ) to be 1.63324(1) Å and 1.63315(1) Å, respectively. The difference in the  $r_e$  values of <sup>202</sup>HgH<sub>2</sub> and <sup>202</sup>HgD<sub>2</sub> is only 0.005% but still an order of magnitude larger than the statistical uncertainties. This discrepancy appears to be due to the breakdown of the Born-Oppenheimer approximation.<sup>46</sup> In contrast, the  $r_e$  distances for different isotopes of mercury are equal within the statistical uncertainties (see Table 3).

TABLE 3: Molecular Constants (in cm<sup>-1</sup>) of <sup>202</sup>HgH<sub>2</sub>, <sup>200</sup>HgH<sub>2</sub>, <sup>202</sup>HgD<sub>2</sub>, and <sup>200</sup>HgD<sub>2</sub>

constant	<sup>202</sup> HgH <sub>2</sub>	<sup>200</sup> HgH <sub>2</sub>	<sup>202</sup> HgD <sub>2</sub>	<sup>200</sup> HgD <sub>2</sub>
<i>B</i> <sub>000</sub>	3.084859(4)	3.084858(4)	1.551156(3)	1.551160(3)
<i>r</i> <sub>0</sub> /Å	1.646543(1) <sup>a</sup>	1.646543(1)	1.642535(2)	1.642534(2)
<i>α</i> <sub>1</sub>	0.04789(3)	0.04790(7)	0.01687(2)	0.01685(2)
<i>α</i> <sub>2</sub>	0.01161(1)	0.01160(2)	0.00412(1)	0.00412(1)
<i>α</i> <sub>3</sub>	0.029828(5)	0.029831(5)	0.010644(4)	0.010649(4)
<i>B</i> <sub>e</sub>	3.135325(24)	3.135316(40)	1.569037(16)	1.569029(19)
<i>r</i> <sub>e</sub> /Å	1.63324(1)	1.63324(1)	1.63315(1)	1.63315(1)
<i>D</i> <sub>e</sub> /10 <sup>-5</sup>	2.76(1)	2.76(3)	0.694(3)	0.694(4)
<i>q</i> <sub>010</sub> /10 <sup>-2</sup>	-4.342(2)	-4.341(3)	-1.5217(7)	-1.5216(9)
<i>ν</i> <sub>3</sub>	1912.81427(6)	1912.90555(6)	1375.78848(8)	1375.91976(9)
<i>x</i> <sub>13</sub>	-70.7901(3)	-70.7915(5)	-35.6712(4)	-35.6738(4)
<i>x</i> <sub>23</sub>	-16.1387(2)	-16.1410(2)	-8.2024(2)	-8.2046(3)
<i>x</i> <sub>33</sub>	-15.1200(1)	-15.1250(1)	-7.3382(2)	-7.3425(2)
<i>ω</i> <sub>1</sub> ( <i>σ</i> <sub>g</sub> )	2112 <sup>b</sup>	2112 <sup>b</sup>	1492 <sup>b</sup>	1492 <sup>b</sup>
<i>ω</i> <sub>2</sub> ( <i>π</i> <sub>u</sub> )	770 <sup>c</sup>	774 <sup>c</sup>		
<i>ω</i> <sub>3</sub> ( <i>σ</i> <sub>u</sub> )	1994.5880(4)	1994.6924(5)	1416.5030(5)	1416.6463(6)

<sup>a</sup> The numbers in parentheses are one standard deviation statistical uncertainties, calculated by propagation of errors. <sup>b</sup> Estimated from *B*<sub>e</sub> and *D*<sub>e</sub> using eq 8. <sup>c</sup> Estimated from *q*<sub>010</sub>, *B*<sub>e</sub> and *ω*<sub>3</sub> using eq 9; the neon matrix values (ref 21) for *ν*<sub>2</sub> of HgH<sub>2</sub> and HgD<sub>2</sub> are 782 cm<sup>-1</sup> and 562 cm<sup>-1</sup>, respectively.

In polyatomic molecules for which equilibrium internuclear distances (*r*<sub>e</sub>) are not available, it is common to calculate the average *r*<sub>s</sub> structure by using the moments of inertia of isotopically substituted molecules. In our previous work on ZnH<sub>2</sub> and ZnD<sub>2</sub>, we calculated the average *r*<sub>s</sub> structure in order to compare it with the *r*<sub>0</sub> and *r*<sub>e</sub> internuclear distances.<sup>46</sup> The ground-state moments of inertia (*I*<sub>0</sub><sup>D</sup> and *I*<sub>0</sub><sup>H</sup>) were calculated from the *B*<sub>000</sub> values of <sup>202</sup>HgD<sub>2</sub> and <sup>202</sup>HgH<sub>2</sub>, respectively, and were used to obtain the average *r*<sub>s</sub> distance by the following equation<sup>50</sup> in which *m*<sub>D</sub> and *m*<sub>H</sub> are the atomic masses for deuterium and hydrogen:

$$I_0^D - I_0^H = 2r_s^2(m_D - m_H) \quad (6)$$

The *r*<sub>s</sub> distance estimated from eq 6 is 1.63851 Å, and lies between the *r*<sub>0</sub> and *r*<sub>e</sub> values.

**3.3. Vibrational Analysis.** A few anharmonicity constants in eq 1 can be calculated directly from the observed band origins (Tables 1 and 2). For <sup>202</sup>HgH<sub>2</sub>, <sup>200</sup>HgH<sub>2</sub>, <sup>202</sup>HgD<sub>2</sub>, and <sup>200</sup>HgD<sub>2</sub> isotopologues, we obtained *x*<sub>13</sub> by taking the difference between the 101 → 100 and 001 → 000 band origins. Similarly, the difference between the 01<sup>1</sup>1 → 01<sup>1</sup>0 and 001 → 000 band origins is equal to *x*<sub>23</sub>, and the difference between the 002 → 001 and 001 → 000 band origins is equal to 2*x*<sub>33</sub> (see eq 1). All of the hot bands of HgH<sub>2</sub> and HgD<sub>2</sub> appeared to lower wavenumbers compared to the *ν*<sub>3</sub> fundamental bands, and thus the *x*<sub>13</sub>, *x*<sub>23</sub>, and *x*<sub>33</sub> constants have negative values (see Table 3). The equilibrium vibrational wavenumber of the antisymmetric stretching mode (*ω*<sub>3</sub>) was then determined using the following equation

$$\nu_3(\text{obs}) = G_{001} - G_{000} = \omega_3 + (1/2)x_{13} + x_{23} + 2x_{33} \quad (7)$$

which is derived from eq 1.

The equilibrium vibrational wavenumber of the symmetric stretching mode (*ω*<sub>1</sub>) was estimated for <sup>202</sup>HgH<sub>2</sub>, <sup>200</sup>HgH<sub>2</sub>, <sup>202</sup>HgD<sub>2</sub>, and <sup>200</sup>HgD<sub>2</sub> isotopologues from *B*<sub>e</sub> and *D*<sub>e</sub> constants, using Kratzer's equation for symmetric linear triatomic molecules:<sup>49</sup>

$$D_e \approx \frac{4B_e^3}{\omega_1^2} \quad (8)$$

The magnitude of the *l*-type doubling constant (*q*) depends on *B*<sub>e</sub>, *ω*<sub>2</sub>, and *ω*<sub>3</sub>, and the following third-order equation can be

used to estimate the *ω*<sub>2</sub> constant:<sup>51</sup>

$$q_{010} \approx \frac{-2B_e^2}{\omega_2} \left( 1 + \frac{4\omega_2^2}{\omega_3^2 - \omega_2^2} \right) \quad (9)$$

For <sup>202</sup>HgH<sub>2</sub> and <sup>200</sup>HgH<sub>2</sub>, we solved eq 9 for *ω*<sub>2</sub> using our *q*<sub>010</sub>, *B*<sub>e</sub> and *ω*<sub>3</sub> values from Table 3. We were unable to determine the *ω*<sub>2</sub> constants of <sup>202</sup>HgD<sub>2</sub> and <sup>200</sup>HgD<sub>2</sub> from eq 9 because the third-order equation for *ω*<sub>2</sub> did not have a solution. However, when we used the neon matrix value of 562 cm<sup>-1</sup> for *ν*<sub>2</sub> of <sup>202</sup>HgD<sub>2</sub> in eq 9, along with our *B*<sub>e</sub> and *ω*<sub>3</sub> values, the predicted *q*<sub>010</sub> constant turned out to be -0.01531 cm<sup>-1</sup>, which differs by less than 1% from the observed value of -0.015217(7) cm<sup>-1</sup>. It should be noted that eqs 8 and 9 are only approximately correct, and the values of *ω*<sub>1</sub> and *ω*<sub>2</sub> obtained from these equations (Table 3) have more than 1% uncertainties.

The absolute vibrational energies of the 100 (*Σ*<sub>g</sub><sup>+</sup>) and 01<sup>1</sup>0 (*Π*<sub>u</sub>) states, that is, *ν*<sub>1</sub> and *ν*<sub>2</sub>, could not be determined from our data. The best ab initio values for *ν*<sub>1</sub> of HgH<sub>2</sub> and HgD<sub>2</sub> are 1982 cm<sup>-1</sup> and 1421 cm<sup>-1</sup>, respectively.<sup>22</sup> The neon matrix values for *ν*<sub>2</sub> of HgH<sub>2</sub> and HgD<sub>2</sub> are 782 cm<sup>-1</sup> and 562 cm<sup>-1</sup>, respectively.<sup>21</sup>

## 4. Discussion

**4.1. Isotope Effects.** The vibrational frequencies for different isotopologues of HgH<sub>2</sub> are related by the following equations:<sup>49</sup>

$$\left( \frac{\omega_1^i}{\omega_1} \right)^2 = \left( \frac{m_H}{m_{H_i}} \right) \quad (10)$$

$$\left( \frac{\omega_2^i}{\omega_2} \right)^2 = \left( \frac{\omega_3^i}{\omega_3} \right)^2 = \left( \frac{m_H}{m_{H_i}} \right) \left( \frac{m_{Hg}}{m_{Hg_i}} \right) \left( \frac{M}{M_i} \right) \quad (11)$$

In the above equations, *m*<sub>H</sub> and *m*<sub>Hg</sub> are the atomic masses of hydrogen (or deuterium) and mercury, respectively, and *M* is the total mass of the molecule. The observed <sup>200</sup>Hg:<sup>202</sup>Hg isotope shift for the *ν*<sub>3</sub> fundamental band of HgH<sub>2</sub> is 0.0913 cm<sup>-1</sup> and corresponds to a ratio of 1.0000477 between the *ν*<sub>3</sub> fundamentals of <sup>200</sup>HgH<sub>2</sub> and <sup>202</sup>HgH<sub>2</sub>. The ratio predicted by eq 11 is 1.0000495. Similarly, the observed <sup>200</sup>Hg:<sup>202</sup>Hg isotope shift for the *ν*<sub>3</sub> fundamental band of HgD<sub>2</sub> is 0.1313 cm<sup>-1</sup>, corresponding

**TABLE 4: Vibrational Wavenumbers and Metal–Hydrogen Internuclear Distances of ZnH<sub>2</sub>, ZnD<sub>2</sub>, CdH<sub>2</sub>, CdD<sub>2</sub>, HgH<sub>2</sub>, and HgD<sub>2</sub>**

molecule	$\nu_3 (\sigma_u)/\text{cm}^{-1}$ gas phase <sup>a</sup>	$\nu_3 (\sigma_u)/\text{cm}^{-1}$ neon matrix	$\nu_2 (\pi_u)/\text{cm}^{-1}$ neon matrix	$r_0/\text{\AA}$ experiment	$r_e/\text{\AA}$ experiment	$r_e/\text{\AA}$ ab initio
<sup>64</sup> ZnH <sub>2</sub>	1889.4326(2) <sup>b</sup>	1880.6 <sup>c</sup>	632.5 <sup>c</sup>	1.535274(2) <sup>b</sup>	1.52413(1) <sup>b</sup>	1.527 <sup>d</sup>
<sup>64</sup> ZnD <sub>2</sub>	1371.6310(2) <sup>b</sup>	1362.6 <sup>c</sup>	456.4 <sup>c</sup>	1.531846(3) <sup>b</sup>	1.52394(1) <sup>b</sup>	1.527 <sup>d</sup>
<sup>114</sup> CdH <sub>2</sub>	1771.5296(2) <sup>e</sup>	1764.1 <sup>c</sup>	604.0 <sup>c</sup>	1.683034(2) <sup>e</sup>		1.668 <sup>d</sup>
<sup>114</sup> CdD <sub>2</sub>	1278.3117(3) <sup>e</sup>	1271.0 <sup>c</sup>	434.5 <sup>c</sup>	1.679172(5) <sup>e</sup>		1.668 <sup>d</sup>
<sup>202</sup> HgH <sub>2</sub>	1912.81427(6)	1918.1 <sup>f</sup>	781.7 <sup>f</sup>	1.646543(1)	1.63324(1)	1.639 <sup>g</sup>
<sup>202</sup> HgD <sub>2</sub>	1375.78848(8)	1378.5 <sup>f</sup>	561.9 <sup>f</sup>	1.642535(2)	1.63315(1)	1.639 <sup>g</sup>

<sup>a</sup> The numbers in parentheses are one standard deviation statistical uncertainties. <sup>b</sup> From ref 46. <sup>c</sup> From ref 56. <sup>d</sup> From ref 20. <sup>e</sup> From ref 45. <sup>f</sup> From ref 21. <sup>g</sup> From ref 22; the best ab initio values for the  $\nu_3$  of HgH<sub>2</sub> and HgD<sub>2</sub> (ref 22) are 1885.66 cm<sup>-1</sup> and 1355.32 cm<sup>-1</sup>, respectively.

to a ratio of 1.0000954 between the  $\nu_3$  fundamentals of <sup>200</sup>HgD<sub>2</sub> and <sup>202</sup>HgD<sub>2</sub>, whereas a ratio of 1.0000979 is predicted by eq 11. The observed ratio between the  $\nu_3$  fundamentals of <sup>202</sup>HgH<sub>2</sub> and <sup>202</sup>HgD<sub>2</sub> (Tables 1 and 2) is 1.3903 and the predicted ratio from eq 11 is 1.4067. If we use our  $\omega_3$  wavenumbers from Table 3 instead, the agreement becomes better and a ratio of 1.4081 is obtained. The observed H:D isotopic ratio for  $\omega_1$  of <sup>202</sup>HgH<sub>2</sub> and <sup>202</sup>HgD<sub>2</sub> (Table 3) is 1.4151, and the predicted ratio from eq 10 is 1.4137.

The  $B_e$ ,  $\alpha_1$ , and  $D_e$  constants of HgH<sub>2</sub> are not sensitive to the mass of mercury, and they should change only when hydrogen is substituted with deuterium.<sup>46</sup> The mass dependences of  $B_e$  and  $\alpha_1$  are given in eqs 4 and 5, and the mass dependence of  $D_e$  is obtained easily by combining eqs 4, 8, and 10. The observed ratios between the  $B_e$ ,  $\alpha_1$ , and  $D_e$  constants of <sup>202</sup>HgH<sub>2</sub> and <sup>202</sup>HgD<sub>2</sub> (Table 3) are 1.99825, 2.840, and 3.984, respectively, whereas the predicted ratios are 1.99846, 2.825, and 3.994, respectively. Equations 4, 9, and 11 can be combined to obtain the mass dependence of the  $l$ -type doubling constant ( $q$ ). The observed ratio between  $q_{010}$  constants of <sup>202</sup>HgH<sub>2</sub> and <sup>202</sup>HgD<sub>2</sub> is 2.8534 and the predicted ratio is 2.8391. Overall, the observed isotope effects are in good agreement with the theoretical predictions. Within the Born–Oppenheimer approximation, all of the isotopologues should have the same equilibrium internuclear distance ( $r_e$ ). We found that  $r_e$  values (Table 3) are the same for different isotopes of mercury, within their experimental uncertainties. The 0.005% difference between the  $r_e$  values of <sup>202</sup>HgH<sub>2</sub> and <sup>202</sup>HgD<sub>2</sub> can be attributed to the breakdown of the Born–Oppenheimer approximation.

**4.2. Comparison with Theory.** A high level ab initio calculation has been performed by Li et al.<sup>22</sup> to obtain the potential energy surface of the  $\tilde{X}^1\Sigma_g^+$  ground electronic state of HgH<sub>2</sub>. They computed the potential energy at 13 000 points using the multireference configuration interaction (MRCI) method with very large basis sets. The potential energy surface was constructed from the ab initio points, and the vibrational energy levels (at  $J = 0$ ) were obtained for HgH<sub>2</sub>, HgHD, and HgD<sub>2</sub> by solving the exact vibration–rotation Schrödinger equation variationally on this surface. The best available theoretical values for the vibrational energy levels of HgH<sub>2</sub>, HgHD, and HgD<sub>2</sub> are thus those obtained by Li and co-workers.<sup>22</sup> However, the  $\nu_3$  values predicted for HgH<sub>2</sub> and HgD<sub>2</sub> in their calculation are 1885.66 cm<sup>-1</sup> and 1355.32 cm<sup>-1</sup>, respectively, whereas the observed  $\nu_3$  values in <sup>202</sup>HgH<sub>2</sub> and <sup>202</sup>HgD<sub>2</sub> in this study are 1912.81427(6) cm<sup>-1</sup> and 1375.78848(8) cm<sup>-1</sup>, respectively (Table 3). It is interesting that even at this high level of theory, the  $\nu_3$  values of HgH<sub>2</sub> and HgD<sub>2</sub> are underestimated by about 27 and 20 cm<sup>-1</sup>, respectively. The equilibrium internuclear distance ( $r_e$ ) predicted by Li et al. is 1.639 Å,<sup>22</sup> which is larger than our experimental  $r_e$  values (Table 3) by about 0.006 Å. Similar ab initio calculations performed by the same group on magnesium dihydride<sup>52</sup> showed somewhat

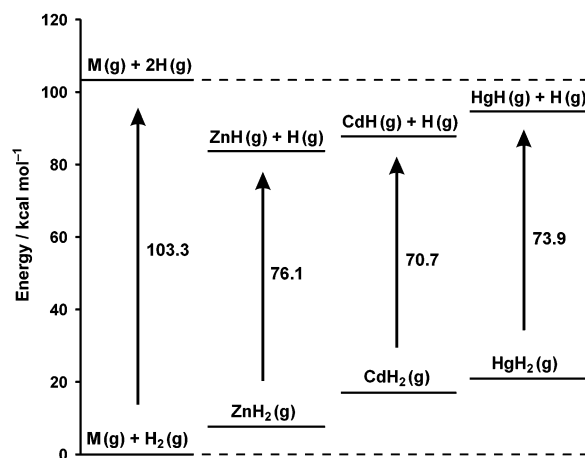
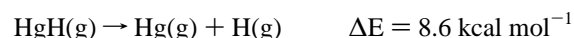
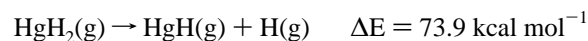


**Figure 4.** Diagram showing the relative energies of gaseous MH and MH<sub>2</sub> molecules (M = Zn, Cd, and Hg). For each metal, the energy of the ground-state M(g) + H<sub>2</sub>(g) was taken as zero.

better agreement with experiment. The theoretical  $\nu_3$  values of MgH<sub>2</sub> and MgD<sub>2</sub> were smaller than the experimental ones<sup>53,54</sup> by about 13 and 10 cm<sup>-1</sup>, respectively.

**4.3. Comparing HgH<sub>2</sub> to ZnH<sub>2</sub> and CdH<sub>2</sub>.** The internuclear distances and vibrational wavenumbers of the most abundant isotopologues of ZnH<sub>2</sub>, ZnD<sub>2</sub>, CdH<sub>2</sub>, CdD<sub>2</sub>, HgH<sub>2</sub>, and HgD<sub>2</sub> are compared in Table 4. The metal–hydrogen internuclear distance in HgH<sub>2</sub> is shorter than that of CdH<sub>2</sub> because of relativistic effects,<sup>13,18</sup> and the vibrational wavenumbers of HgH<sub>2</sub> are larger than those of ZnH<sub>2</sub> and CdH<sub>2</sub>. A combination of experimental and theoretical data can be used to estimate the dissociation energies of the Hg–H bonds in gaseous HgH<sub>2</sub>. High level ab initio calculations<sup>22</sup> predicted that the gas-phase reaction Hg(g) + H<sub>2</sub>(g) → HgH<sub>2</sub>(g) is endoergic by 20.8 kcal mol<sup>-1</sup> for ground-state mercury atoms. The experimental values for dissociation energies of H<sub>2</sub> and HgH are 103.3 and 8.6 kcal mol<sup>-1</sup>, respectively,<sup>55</sup> and it is straightforward to calculate that the dissociation energy of the first Hg–H bond in HgH<sub>2</sub> is 73.9 kcal mol<sup>-1</sup>, significantly larger than that of the second bond



Similar patterns exist in the bond energies of gaseous ZnH<sub>2</sub> and CdH<sub>2</sub>, suggesting that average bond strengths should not be used to discuss bonding in these molecules. The best ab initio values for the heats of formation of gaseous ZnH<sub>2</sub> and CdH<sub>2</sub> from ground-state metal atoms and molecular hydrogen are +7.6 and +17.0 kcal mol<sup>-1</sup>, respectively,<sup>20</sup> and the experimental values for the dissociation energies of ZnH and CdH are 19.6 and 15.6 kcal mol<sup>-1</sup>, respectively.<sup>55</sup> Therefore, the dissociation energies of the first metal–hydrogen bond in gaseous ZnH<sub>2</sub> and



CdH<sub>2</sub> are estimated to be 76.1 and 70.7 kcal mol<sup>-1</sup>, respectively. The relative energies of gaseous MH and MH<sub>2</sub> molecules (M = Zn, Cd, and Hg) are compared in a simple diagram in Figure 4.

## 5. Conclusions

High-resolution infrared emission spectra of gaseous HgH<sub>2</sub> and HgD<sub>2</sub> in the  $\nu_3$  region were analyzed for six naturally abundant isotopes of mercury. The  $\nu_3$  fundamentals of <sup>202</sup>HgH<sub>2</sub>, <sup>200</sup>HgH<sub>2</sub>, <sup>202</sup>HgD<sub>2</sub>, and <sup>200</sup>HgD<sub>2</sub> were observed at 1912.81427(6), 1912.90555(6), 1375.78848(8), and 1375.91976(9) cm<sup>-1</sup>, respectively, and the mercury isotope shifts were consistent with the theoretical predictions of eq 11. In addition to the  $\nu_3$  fundamental bands of <sup>204</sup>HgH<sub>2</sub>, <sup>202</sup>HgH<sub>2</sub>, <sup>201</sup>HgH<sub>2</sub>, <sup>200</sup>HgH<sub>2</sub>, <sup>199</sup>HgH<sub>2</sub>, <sup>198</sup>HgH<sub>2</sub>, <sup>204</sup>HgD<sub>2</sub>, <sup>202</sup>HgD<sub>2</sub>, <sup>201</sup>HgD<sub>2</sub>, <sup>200</sup>HgD<sub>2</sub>, <sup>199</sup>HgD<sub>2</sub>, and <sup>198</sup>HgD<sub>2</sub>, a few hot bands involving  $\nu_1$ ,  $\nu_2$ , and  $\nu_3$  were assigned and analyzed rotationally to determine spectroscopic constants. Using the rotational constants of the 000, 100, 01<sup>1</sup>0, and 001 vibrational levels, the equilibrium rotational constants ( $B_e$ ) of the most abundant isotopologues, <sup>202</sup>HgH<sub>2</sub> and <sup>202</sup>HgD<sub>2</sub>, were determined to be 3.135325(24) cm<sup>-1</sup> and 1.569037(16) cm<sup>-1</sup>, respectively, and the associated equilibrium Hg–H and Hg–D internuclear distances ( $r_e$ ) are 1.63324(1) Å and 1.63315(1) Å, respectively. The  $r_e$  distances of <sup>202</sup>HgH<sub>2</sub> and <sup>202</sup>HgD<sub>2</sub> differ by about 0.005%, which can be attributed to the breakdown of the Born–Oppenheimer approximation.

**Acknowledgment.** This project was supported financially by the Natural Sciences and Engineering Research Council (NSERC) of Canada.

**Supporting Information Available:** A complete list of the observed line positions and the outputs of least-squares fitting program (Tables 1S–12S). This material is available free of charge via the Internet at <http://pubs.acs.org>.

## References and Notes

- (1) Stokstad, E. *Science* **2004**, *303*, 34.
- (2) Lu, D. Y.; Granatstein, D. L.; Rose, D. J. *Ind. Eng. Chem. Res.* **2004**, *43*, 5400.
- (3) Schroeder, W. H.; Munthe, J. *Atmos. Environ.* **1998**, *32*, 809.
- (4) Stein, E. D.; Cohen, Y.; Winer, A. M. *Crit. Rev. Environ. Sci. Technol.* **1996**, *26*, 1.
- (5) Mason, R. P.; Morel, F. M. M.; Hemond, H. F. *Water, Air, Soil Pollut.* **1995**, *80*, 775.
- (6) Barkay, T.; Miller, S. M.; Summers, A. O. *FEMS Microbiol. Rev.* **2003**, *27*, 355.
- (7) Hatch, W. R.; Ott, W. L. *Anal. Chem.* **1968**, *40*, 2085.
- (8) Sturgeon, R. E.; Mester, Z. *Appl. Spectrosc.* **2002**, *56*, 202A.
- (9) Feng, Y.-L.; Sturgeon, R. E.; Lam, J. W. *Anal. Chem.* **2003**, *75*, 635.
- (10) Filippelli, M.; Baldi, F.; Brinckman, F. E.; Olson, G. J. *Environ. Sci. Technol.* **1992**, *26*, 1457.
- (11) Weber, J. H. *Mar. Chem.* **1999**, *65*, 67.
- (12) Thayer, J. S. *Environmental Chemistry of the Heavy Elements: Hydrido and Organo Compounds*; VCH: New York, 1995.
- (13) Pyykkö, P. *J. Chem. Soc., Faraday Trans. 2* **1979**, *75*, 1256.
- (14) Dolg, M.; Küchle, W.; Stoll, H.; Preuss, H.; Schwerdtfeger, P. *Mol. Phys.* **1991**, *74*, 1265.
- (15) Schwerdtfeger, P.; Heath, G. A.; Dolg, M.; Bennet, M. A. *J. Am. Chem. Soc.* **1992**, *114*, 7518.
- (16) Schwerdtfeger, P.; Boyd, P. D. W.; Brienne, S.; McFeaters, J. S.; Dolg, M.; Liao, M.-S.; Schwarz, W. H. E. *Inorg. Chim. Acta* **1993**, *213*, 233.
- (17) Kaupp, M.; von Schnering, H. G. *Inorg. Chem.* **1994**, *33*, 2555.
- (18) Kaupp, M.; von Schnering, H. G. *Inorg. Chem.* **1994**, *33*, 4179.
- (19) Pyykkö, P.; Straka, M.; Patzschke, M. *Chem. Commun.* **2002**, 1728.
- (20) Greene, T. M.; Brown, W.; Andrews, L.; Downs, A. J.; Chertihin, G. V.; Runeberg, N.; Pyykkö, P. *J. Phys. Chem.* **1995**, *99*, 7925.
- (21) Wang, X.; Andrews, L. *Phys. Chem. Chem. Phys.* **2005**, *7*, 750.
- (22) Li, H.; Xie, D.; Guo, H. *J. Chem. Phys.* **2005**, *122*, 144314.
- (23) von Szentpály, L. *J. Phys. Chem. A* **2002**, *106*, 11945.
- (24) Burns, K.; Adams, K. B.; Longwell, J. J. *Opt. Soc. Am.* **1950**, *40*, 339.
- (25) Breckenridge, W. H.; Jouvet, C.; Soep, B. *J. Chem. Phys.* **1986**, *84*, 1443.
- (26) Bras, N.; Butaux, J.; Jeannot, J. C.; Perrin, D. *J. Chem. Phys.* **1986**, *85*, 280.
- (27) Bernier, A.; Millie, P. *Chem. Phys. Lett.* **1987**, *134*, 245.
- (28) Bernier, A.; Millie, P. *J. Chem. Phys.* **1988**, *88*, 4843.
- (29) Bras, N.; Jeannot, J. C.; Butaux, J.; Perrin, D. *J. Chem. Phys.* **1991**, *95*, 1006.
- (30) Siegbahn, P. E. M.; Svensson, M.; Crabtree, R. H. *J. Am. Chem. Soc.* **1995**, *117*, 6758.
- (31) Ohmori, K.; Takahashi, T.; Chiba, H.; Saito, K.; Nakamura, T.; Okunishi, M.; Ueda, K.; Sato, Y. *J. Chem. Phys.* **1996**, *105*, 7464.
- (32) Breckenridge, W. H. *J. Phys. Chem.* **1996**, *100*, 14840.
- (33) Wiberg, E.; Henle, W. *Z. Naturforsch.* **1951**, *6b*, 461.
- (34) Wiberg, E. *Angew. Chem.* **1953**, *65*, 16.
- (35) Mueller, W. M.; Blackledge, J. P.; Libowitz, G. G. *Metal Hydrides*; Academic Press: New York, 1968.
- (36) Wang, X.; Andrews, L. *Inorg. Chem.* **2004**, *43*, 7146.
- (37) Aldridge, S.; Downs, A. J. *Chem. Rev.* **2001**, *101*, 3305.
- (38) Andrews, L. *Chem. Soc. Rev.* **2004**, *33*, 123.
- (39) Legay-Sommaire, N.; Legay, F. *Chem. Phys. Lett.* **1993**, *207*, 123.
- (40) Legay-Sommaire, N.; Legay, F. *J. Phys. Chem.* **1995**, *99*, 16945.
- (41) Macrae, V. A.; Greene, T. M.; Downs, A. J. *Phys. Chem. Chem. Phys.* **2004**, *6*, 4586.
- (42) Wang, X.; Andrews, L. *Inorg. Chem.* **2005**, *44*, 108.
- (43) Shayesteh, A.; Yu, S.; Bernath, P. F. *Chem.—Eur. J.* **2005**, *11*, 4709.
- (44) Shayesteh, A.; Appadoo, D. R. T.; Gordon, I. E.; Bernath, P. F. *J. Am. Chem. Soc.* **2004**, *126*, 14356.
- (45) Yu, S.; Shayesteh, A.; Bernath, P. F. *J. Chem. Phys.* **2005**, *122*, 194301.
- (46) Shayesteh, A.; Gordon, I. E.; Appadoo, D. R. T.; Bernath, P. F. *Phys. Chem. Chem. Phys.* **2005**, *7*, 3132.
- (47) Maki, A. G.; Wells, J. S. *Wavenumber Calibration Tables from Heterodyne Frequency Measurements*; NIST Special Publication 821, U.S. Government Printing Office: Washington, DC, 1991.
- (48) Bernath, P. F. *Spectra of Atoms and Molecules*, 2nd ed.; Oxford University Press: New York, 2005.
- (49) Herzberg, G. *Molecular Spectra and Molecular Structure II. Infrared and Raman Spectra of Polyatomic Molecules*; Krieger: Malabar, FL, 1991.
- (50) Chutjian, A. *J. Mol. Spectrosc.* **1964**, *14*, 361.
- (51) Watson, J. K. G. *Can. J. Phys.* **2001**, *79*, 521.
- (52) Li, H.; Xie, D.; Guo, H. *J. Chem. Phys.* **2004**, *121*, 4156.
- (53) Shayesteh, A.; Appadoo, D. R. T.; Gordon, I.; Bernath, P. F. *J. Chem. Phys.* **2003**, *119*, 7785.
- (54) Shayesteh, A.; Appadoo, D. R. T.; Gordon, I.; Bernath, P. F. *Can. J. Chem.* **2004**, *82*, 947.
- (55) Huber, K. P.; Herzberg, G. *Molecular Spectra and Molecular Structure IV. Constants of Diatomic Molecules*; Van Nostrand: New York, 1979.
- (56) Wang, X.; Andrews, L. *J. Phys. Chem. A* **2004**, *108*, 11006.